NASA Technical Memorandum 107456

Thin Film Multilayer Conductor/Ferroelectric Tunable Microwave Components for Communication Applications

Félix A. Miranda, Robert R. Romanofsky and Frederick W. Van Keuls
Lewis Research Center
Cleveland, Ohio

Carl H. Mueller, Randolph E. Treece, and Tania V. Rivkin
SCT
Golden, Colorado

Prepared for the
9th International Symposium on Integrated Ferroelectrics
sponsored by the University of Colorado
Santa Fe, New Mexico, March 2–5, 1997

National Aeronautics and
Space Administration

THIN FILM MULTILAYER CONDUCTOR/FERROELECTRIC TUNABLE MICROWAVE COMPONENTS FOR COMMUNICATION APPLICATIONS

FELIX A. MIRANDA[a], ROBERT R. ROMANOFSKY[a], FREDERICK W. VAN KEULS[a], CARL H. MUELLER[b], RANDOLPH E. TREECE[b], and TANIA V. RIVKIN[b]
[a]NASA Lewis Research Center, Cleveland, Ohio, 44135, USA;
[b]SCT, Golden, Colorado, 80401, USA

A study of Au/$SrTiO_3$/$YBa_2Cu_3O_{7-\delta}$/$LaAlO_3$ and (Au,$YBa_2Cu_3O_{7-\delta}$)/$Ba_xSr_{1-x}TiO_3$/$LaAlO_3$ (x=0, 0.50, and 0.40) multilayered structures is presented. At 1.0 MHz, the largest tuning of Au/$SrTiO_3$/$YBa_2Cu_3O_{7-\delta}$ parallel plate capacitors corresponded to single-phased, epitaxial 300-500 nm thick $SrTiO_3$ thin films deposited at 800 °C. For $SrTiO_3$/$LaAlO_3$ structures having $SrTiO_3$ films of similar quality, we observed that at 1.0 MHz and 77 K, interdigital capacitors exhibit higher tunabilities and lower losses than parallel plate configurations, but required higher dc voltage. For a 300 nm thick $SrTiO_3$ film, a 25 Ω $YBa_2Cu_3O_{7-\delta}$/$SrTiO_3$/$LaAlO_3$ phase shifter exhibited a phase shift ~2.6 times larger than its Au/$SrTiO_3$/$LaAlO_3$ counterpart. At 19 GHz and 32 V, a 360° phase shift could in principle be achieved with coupled microstripline sections only 7.0 mm long. At 14 GHz, 77 K and 260 V, for 1.0 μm and 300 nm thick $SrTiO_3$ films, 25 Ω 360° Au/$SrTiO_3$/$LaAlO_3$ phase shifters would be nominally 4.0 mm and 12 mm long, respectively. For a 2λ $YBa_2Cu_3O_{7-\delta}$ $SrTiO_3$/$LaAlO_3$ ring resonator a tuning rate of 0.7 MHz/Volt was achieved at 10 GHz and 77 K. The relevance of these structures for phased array antennas and as tunable elements in discriminator-stabilized oscillators is discussed.

Keywords: (HTS,metal)/ferroelectric structures; tunable microwave components; dielectric constant; loss tangent; parallel plate and interdigital capacitors; phase shifters; ring resonators.

INTRODUCTION

Improvements in the quality of ferroelectric thin films have prompted their usage in proof-of-concept (POC) tunable microwave components such as varactors, phase shifters, and filters, amongst others.[1-3] For practical microwave applications, issues such as optimization of the dielectric properties of the ferroelectric films, device configuration (i.e., parallel or interdigital), and degree of tunability versus losses, amongst others, must be addressed.

In the area of satellite communications, congestion of the frequency spectrum at and below the Ku-band resulting from the boom of the wireless communication industry, has prompted utilization of higher frequency bands such as the K- and Ka-band. Phased array antennas have been identified as a critical component for many of the proposed satellite constellations (e.g., Teledesic) targeted for operation by the turn of the century[4]. Hence, compact, low loss phase shifters will be an enabling component for these applications. In addition, small, low cost, low-phase noise local oscillators (LO) which are compatible with high order, bandwidth efficient modulation schemes (e.g., QPSK) are required.

In this paper, we report on our study of gold/$SrTiO_3$/$YBa_2Cu_3O_{7-\delta}$/$LaAlO_3$(Au/STO/YBCO/LAO) and (gold,$YBa_2Cu_3O_{7-\delta}$)/$Ba_xSr_{1-x}TiO_3$/$LaAlO_3$(x=0, 0.50, and 0.40) ((Au,YBCO)/BSTO/LAO) multilayered structures. The effect of the deposition temperature of the ferroelectric film on the tuning and losses of parallel plate capacitors at 1.0 MHz is discussed. Dependence of tuning and losses on the geometry of the tunable components is presented. As a demonstration of the great potential of these components for advantageous insertion into satellite and ground-based communication systems, we present results of proof-of-concept (POC) coupled microstripline phase shifters (CMPS) and interdigital ring resonators for LO between the 10-20 GHz frequency range.

EXPERIMENTAL

The multilayer structures considered in this study were deposited in-situ on (100) LAO single-crystal substrates (254 and 508 μm thick) by pulsed laser deposition (PLD). The dielectric properties of the STO films in the Au/STO/YBCO parallel plate configuration were studied by varying the deposition temperature of the ferroelectric film from 825° to 250 °C. For all these structures the YBCO films were deposited at 800 °C. For this part of the study, the STO films were 300-500 nm thick, and the YBCO films were ~350 nm thick. The parallel plate capacitor used in this study is similar to that used previously;[5,6] Au electrodes (~2.5 μm thick) were used. For the interdigital configurations we used Au and platinum (Pt) electrodes, 0.5 μm thick. In this configuration we also examined BSTO films which were also deposited by PLD and were ~500 nm thick. The electrodes were deposited by electron beam (e-beam) evaporation. A 15 nm thick titanium or chromium adhesion layer was e-beam evaporated before the metal deposition. Standard photolithography techniques and chemical etching (lift-off) were used to fabricate these structures. The crystal structure and surface topology of the ferroelectric films were analyzed by X-Ray Diffraction (XRD) and Atomic Force Microscopy (AFM), respectively.

At low frequencies (i.e., 1.0 MHz), the electrical response of the multilayer structures was studied by measuring the dielectric constant (ε_r) and loss tangent ($\tan\delta$) of the ferroelectric film as a function of temperature (300-20 K), at ac voltages within 5-100 mV, and at dc electric fields from zero to 1.0×10^5 V/cm for the parallel plate capacitors, and up to 3.5×10^5 V/cm for the interdigital configurations. An HP 4192A LF Impedance Analyzer coupled through bias lines to the second stage of a closed-cycle helium gas refrigerator was used to perform these measurements. The measurement system was fully automated and controlled by an HP 900-300 computer. Characterization of the coupled microstripline phase shifters and the interdigital ring resonators at frequencies between 10-20 GHz was performed using an HP 8510C automatic network analyzer (ANA) coupled through semi-rigid input/output coaxial cables to the second stage of a closed-cycle helium gas refrigerator similar to the one mentioned above. All the measurements were performed under a vacuum of less than 10 mtorr.

RESULTS

Figure 1 shows data on ε_r and tanδ for a Au/STO/YBCO parallel plate capacitor with the STO film deposited at 800 °C. The area for the Au electrodes was 400×400 μm^2 and the STO film was 300 nm thick. In this study we found that the largest tuning corresponds to the structures with the 800 °C STO films. As reported previously, we have observed that higher deposition temperatures resulted in interfacial degradation and poor film quality, while lower deposition temperatures resulted in films with lower dielectric constants, lower tunabilities, and higher losses.[7] Similar results were also obtained for film thicknesses near 500 nm. For STO films deposited at temperatures near 800 °C, XRD scans showed that the films were (100) oriented and singled-phased. Thus, maximum tuning of the Au/STO/YBCO structure can be attained with single-phased, epitaxial 300-500 nm thick STO films deposited at 800 °C. As shown in figure 1, the tanδ for these films was typically ~0.05 for temperatures below 80 K, and was insensitive to changes in dc bias. However, we have observed that the parallel plate structure is influenced by electrical shorts in the ferroelectric film which are in turn associated with the roughness of the YBCO film.[6,8] Thus, improving the smoothness of the underlying YBCO layer may help in reducing the electrical shorts in the ferroelectric layers.

The dielectric properties of the interdigital structures investigated were significantly different from those of the parallel plate capacitors. Several capacitor dimensions were studied; in general the gaps between the electrodes and the finger width were either 10 or 20 μm, the number of

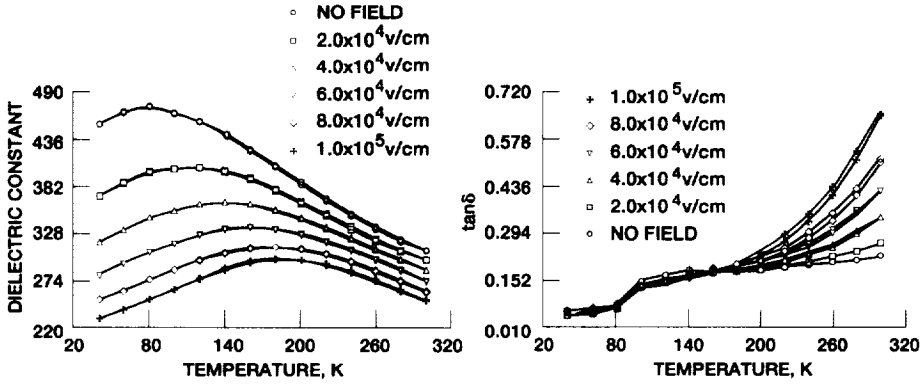

Figure 1 Dependence of ε_r and tanδ on temperature and applied dc field for the STO film in a Au/STO/YBCO parallel plate capacitor. The STO film (300 nm) was deposited at 800 °C. The YBCO and Au electrodes are 350 nm thick and 2.5 μm thick, respectively. Data are shown for the cooling and warming cycles and were taken at 1.0 MHz. The contact area was 400 μm x 400 μm.

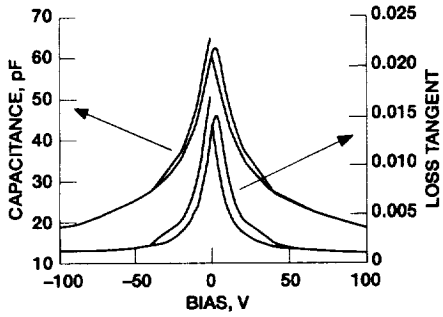

FIGURE 2 Capacitance and tanδ as a function of dc voltage for an interdigital Au/STO/LAO structure. The data were taken at 1.0 MHz.

interdigital fingers varied from 13 to 50, and the finger length was always 1.0 mm. Figure 2 shows the capacitance and tanδ of a Au/STO/LAO interdigital capacitor at 77 K and 1.0 MHz. Note that the degree of tuning and the tanδ values are larger and smaller, respectively, than those corresponding to parallel plate capacitors, although larger values of dc bias are required for the interdigital configuration. For example, a tuning of 47% was attained at 80 K for the sample shown in figure 1 by applying a dc bias of just 5 V, while for the interdigital capacitor a tunability of 70% was observed at a dc voltage of 50 V. The loss behavior of the STO film in the interdigital structure was attributed to defects intrinsic to the STO whereas for the film in the parallel plate capacitor they were mainly dominated by electrical shorts of the YBCO through the STO film. Figure 3 shows the capacitance as a function of temperature and dc bias for Au/STO/LAO and Pt/BSTO/LAO (Ba:Sr;0.50:0.50) interdigital capacitors at 1.0 MHz. Observe that the point of maximum tuning

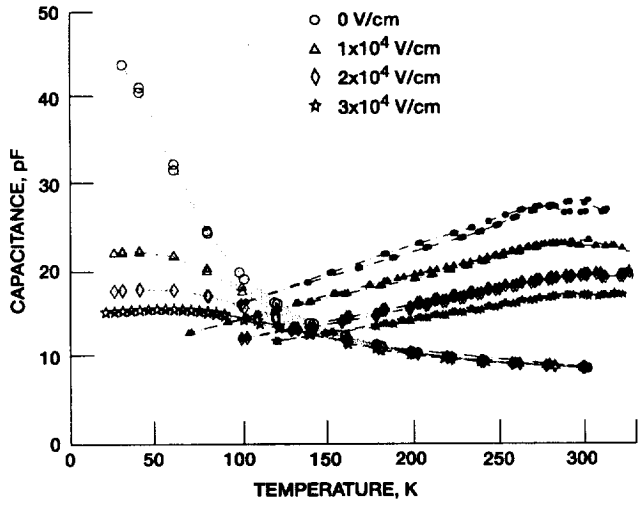

FIGURE 3 Capacitance versus temperature, for several electric field intensities, for a Au/STO/LAO interdigital capacitor (open symbols) and a Pt/BSTO/LAO interdigital capacitor (solid symbols). The data were taken at 1.0 MHz.

occurs at different temperatures. Therefore, applications at cryogenic temperatures could in principle be realized using STO films while those targeted for temperatures near or at room temperature could potentially be realized by using BSTO films.

Most of the studies on ferroelectric based structures heretofore have been performed at low frequencies. Table I shows a summary of some of these works, which provide data on ε_r, tanδ, type of structure, percent of tunability $(((\varepsilon_r(0) - \varepsilon_r(V_{max}))/ \varepsilon_r(0))\times 100 = (\Delta\varepsilon_r/\varepsilon_r(0))\times 100)$, and K-factor $((\Delta\varepsilon_r/\varepsilon_r(0))/\tan\delta(0))$, amongst others. The K-factor is a figure of merit that allows the comparison of different samples in a meaningful way. Therefore, as part of our study we have examined the performance of the (Au,HTS)/STO/LAO structures at K-band frequencies. Figure 4 shows a schematic diagram of a 25 Ω (with input/output 50 to 25 Ω transformers), and 50 Ω CMPS. For these phase shifters, the line capacitance was calculated by adapting the quasi-TEM variational expression of Koul and Bhat,[9] and using the transmission line method of Crampagne, Ahmadpanah, and Guiraud.[10] The coupled line structure was optimized to minimize loss and maximize phase shift. In doing so, we tried to capitalize in the fact that the thin ferroelectric film is most effective when the phase velocity (V_p) is dominated by the odd mode fields. The propagation constant is given by,

$$\beta = \omega/V_p = (\pi/\lambda_o)[(\varepsilon_{even})^{0.5}+(\varepsilon_{odd})^{0.5}] \qquad (1)$$

where, λ_o is the free space wavelength, $\varepsilon_{even} = C_E/C_{Eair}$ and $\varepsilon_{odd} = C_O/C_{Oair}$, and C_{Eair} and C_{Oair} are obtained by replacing all dielectrics with air. Thus, by capitalizing on the odd mode propagation constant, coupled microstripline phase shifters could yield more phase shift per

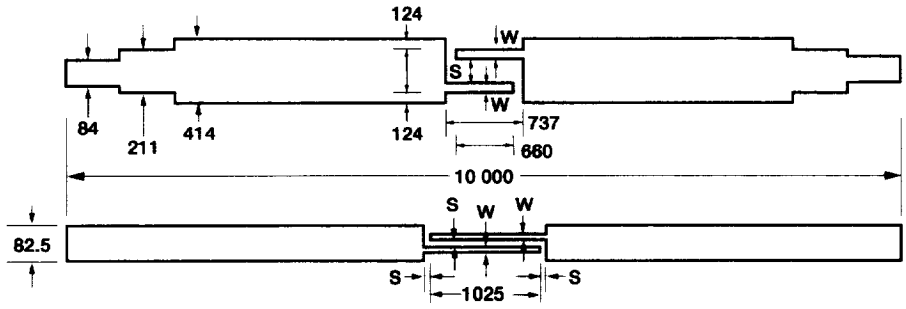

FIGURE 4 Au(1.5 μm thick)/STO/LAO(254 μm thick), microstrip transmission line with 20 GHz bandpass interdigital section (with input/output 50 to 25 Ohms transformers). S = 12.7 μm, W = 76.2 μm. Bottom; S = 7.5 μm, W = 25 μm. All dimensions are in microns.

TABLE I Ferroelectric based structures.

Material	Electrode	Temp. (K)	ϵ_r	tanδ	frequency, (GHz)	% tunability	K factor	Type of capacitor	E (10^4 V/cm)	Volts	Reference
BSTO 0.45:0.55 Ceramic 508 μm thick		298	800	0.09	4.0				0	0	Babbitt, et al., Mic. Jour. 53, 1992
BSTO 0.6:0.4, PLD films, 0.6 μm thick	Pt, RuO_2	298	1200 924		0.5×10^{-3}	23		parallel plate Pt/BSTO/ RuO_2	0 3.0	0 1.8	L.C. Sengupta et al., Army Science Conf., 1996
BSTO 0.6:0.4, PLD films, 0.6 μm, Oxide III doped	Pt, RuO_2	298	926 722		0.5×10^{-3}	22		parallel plate Pt/BSTO/ RuO_2	0 3.0	0 1.8	L.C. Sengupta et al., Army Science Conf., 1996
BSTO 0.6:0.4, MOD films, 0.4 μm thick	Pt, RuO_2	298	450 357	0.013	0.5×10^{-3}	20.7	15.9	parallel plate Pt/BSTO/ RuO_2	0 10	0 4	L.C. Sengupta et al., Army Science Conf., 1996
BSTO 0.6:0.4, MOD films, 0.4 μm thick, Oxide III doped	Pt, RuO_2	298	386 337	0.007	0.5×10^{-3}	12.7	18	parallel plate Pt/BSTO/ RuO_2	0 10	0 4	L.C. Sengupta et al., Army Science Conf., 1996
BSTO 0.6:0.4, Polycrystalline ceramic, 30% oxide III	Pt, RuO_2	298	646	0.0040	2.139			parallel plate Pt/BSTO/ RuO_2	0	0	L.C. Sengupta et al., Army Science Conf., 1996
BSTO 0.6:0.4, Polycrystalline ceramic 40% Oxide III	Pt, RuO_2	298	404	0.0042	1.815			parallel plate Pt/BSTO/ RuO_2	0	0	L.C. Sengupta et al., Army Science Conf., 1996
BSTO 0.6:0.4, Polycrystalline ceramic 60%	Pt, RuO_2	298	113	0.0065	4.581			parallel plate Pt/BSTO/ RuO_2	0	0	L.C. Sengupta et al., Army Science Conf., 1996
KTO, 0.3 μm thick, PLD films	Ag/YBCO	298	270	0.01	1×10^{-4}			parallel plate	0	0	Boikov, et al., Supercon. Sci. Tech. 9, 1996
KTO, 0.3 μm thick, PLD films	Ag/YBCO	77	410 370	0.007 0.007	1×10^{-4}	9.8	13.9	parallel plate	6.67	0 2.0	Boikov, et al., Supercon. Sci. Tech. 9, 1996
STO, 0.3 μm thick, PLD films	Ag/YBCO	298 54	270 400 max.	0.018 0.015	1×10^{-4}			parallel plate	0 0	0 0	Boikov, et al., Supercon. Sci. Tech. 9, 1996

TABLE I Concluded.

Material	Electrode	Temp. (K)	ε_r	tanδ	frequency, (GHz)	% tunability	K factor	Type of capacitor	E (10^4 V/cm)	Volts	Reference
BSTO 0.25:0.75,3 μm thick, PLD films	YBCO	298 130	300 350 max	0.019 0.016	1×10^{-4}				0 0	0 0	Boikov, et al., Supercon. Sci. Tech. 9, 1996
BSTP, 0.1:0.9, pellet, 0.71 mm thick	YBCO	86	30,000 5,000	0.026 0.005	1×10^{-4}	83	31.9	coplanar slot capacitor	0 2.5	0 200	H-D Wu, et al. IEEE Trans. Appl. Sup. 4, 1994
BSTO, 0.08:0.92, 0.3 μm thick, MOD films	YBCO (PLD)	70	258 200	0.029 0.025	1×10^{-4}	22.5	7.8	Interdig. BSTO/YB CO/LAO	0 6.6	0 50	H-D Wu, et al. IEEE Trans. Appl. Sup. 4, 1994
STO, 2.0 μm thick, PLD films	YBCO	298 30 10	300 1600 1500		1×10^{-5}			CPW, YBCO/STO/ LAO	0	0	Findikoglu et al., 1996 ASC
BSTO 0.6:0.4, 0.3 μm thick, PLD films	Pt, RuO_2	298	1260 970		1×10^{-3}	23		parallel plate capacitor (Al_2O_3 is the substrate)	0 3.0	0 0.9	S. Sengupta, et al., ARL-TR-754 1995
BSTO 0.6:0.4, 0.3 μm thick, PLD films, 1% Oxide III	Pt, RuO_2	298	735 559		1×10^{-3}	24		Parallel plate capacitor	0 3.0	0 0.9	S. Sengupta, et al., ARL-TR-754 1995
BSTO 0.6:0.4, pellet, 1 mm thick	Pt	298	3,300 2,640		1×10^{-3}	20		Parallel plate capacitor	0 0.73	0 730	S. Sengupta, et al., ARL-TR-754 1995
BSTO 0.6:0.4, 1 mm thick pellets, 1% Oxide III	Pt	298	1,276 1,072		1×10^{-3}	16		Parallel plate capacitor	0 2.32	0 2,320	S. Sengupta, et al., ARL-TR-754 1995
STO, 0.8 μm thick, PLD films	YBCO	77	1,150 300	0.1	1.2×10^{-7}	74	7.4	Parallel plate capacitor	0 10	0 8	Findikoglu et al., Appl. Phys. Lett. 63, 1993
STO, 550 nm thick, PLD film	YBCO	4	920 330	0.05	11	64	12.8	coplanar capacitor	0 8	0 40	D. Galt, et al., Appl. Phys. Lett., 63, 1993
BSTO, 0.6:0.4, 112 μm thick, tape casting	Au/Pd/Pt	298	3,192.2	0.0056	1×10^{-6}	43.52		coplanar capacitor	2.0	224	L.C. Sengupta, et al. ARL-TR-753, 1995

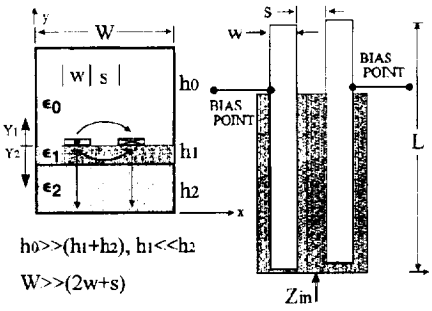

FIGURE 5 Coupled microstripline ferroelectric phase shifter.

unit length than simple microstrip lines while avoiding the need for a coplanar ground. The schematic shown in figure 5 summarizes our design approach.

Figure 6 shows experimental data, measured at 77 K and 19.4 GHz, for Au/STO(300 nm)/LAO and YBCO/STO(300 nm)/LAO CMPS. Note that a relative insertion phase shift ($\Delta\phi$) of ~13° is attained with a dc bias of 32 V (2.5×10^4 V/cm). By replacing the Au layer with a YBCO film, we obtained $\Delta\phi$~34° at the same temperature, frequency and field. The raw insertion loss was less than 3 dB. Since the coupling length of the CMPS is 0.66 mm, this result implies that at 19 GHz and 32 V, a 360° phase shift could in principle be achieved with coupled microstripline sections only 7.0 mm long. Since this configuration relies in the odd mode propagation of the field across the ferroelectric film, we decided to investigate $\Delta\phi$ for thicker STO films. Figure 7 shows $\Delta\phi$ versus dc bias for Au/STO/LAO CMPS with 500 nm and 1.0 μm thick STO films. Note that for both samples there is a reversal of $\Delta\phi$ at a specific bias. This phase reversal can be explained in terms of change in ε_r with applied field. By modeling the structure using Sonnet em®

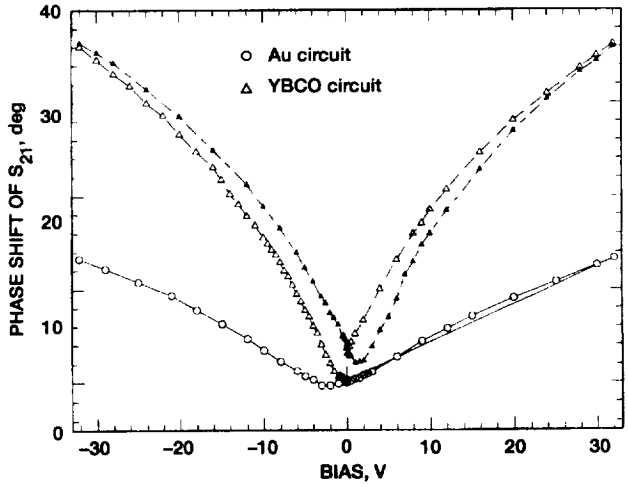

FIGURE 6 Au(1.5 μm)/STO(300nm)/LAO(254 μm) and YBCO(350 nm)/STO(300 nm)/LAO(254 μm) 25 Ω coupled microstripline phase shifters. Open (solid) symbols denote increasing (decreasing) bias. The data were taken at 19.4 GHz.

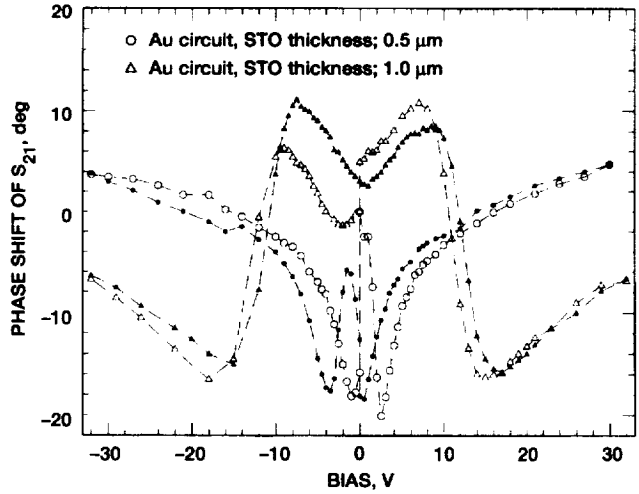

FIGURE 7 Au(1.5 μm)/STO/LAO(254 μm) 25 Ω coupled microstripline phase shifters. Open (solid) symbols denote increasing (decreasing) bias. The data were taken at 20.455 GHz.

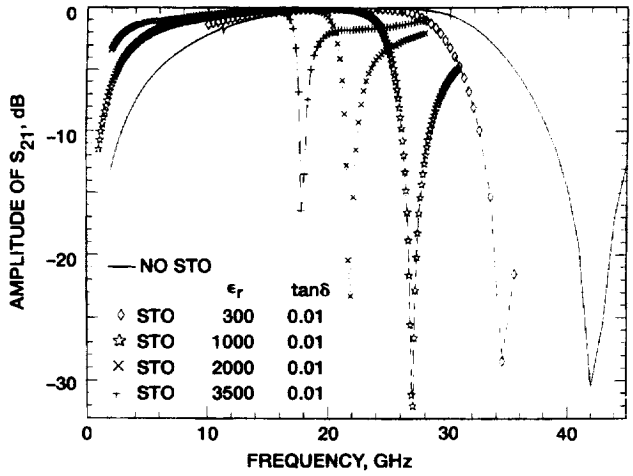

FIGURE 8 Au(1.5 μm)/STO(300nm)/LAO(254 μm) 50 Ω coupled microstripline phase shifters: Sonnet em® simulation.

simulator, one can see that the bandpass of the CMPS is very broad in the absence of STO (see figure 8). Adding the STO layer ($\epsilon_r = 300$) to the structure, results in a narrowing of the passband, which compresses even more as the structure is cooled to cryogenic temperatures and ϵ_r for the STO layer increases ($\epsilon_r \sim 3500$). Applying the dc bias results in lower values of ϵ_r with the concomitant shifting of the band edge to higher frequencies. Thus, the observed $\Delta\phi$ reversal for the 500 nm and 1.0 μm films, results from the frequency of operation being at the band

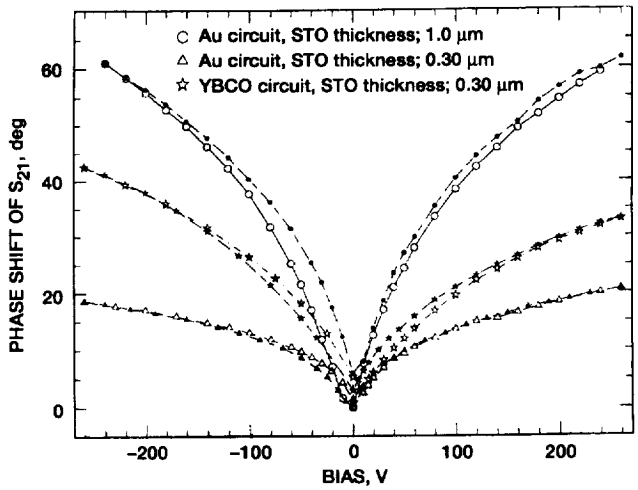

FIGURE 9 25 Ω coupled microstripline phase shifters; T = 77K, frequency = 13.73 GHz. Open (solid) symbols denote increasing (decreasing) bias.

edge of the CMPS passband for a given bias value within the bias range considered in this study. Hence, for the CMPS under consideration one must be careful to operate within the passband, or at frequencies where the passband is insensitive to changes in ε_r; figure 8 suggests that frequencies near 14 GHz could satisfy this criteria. Figure 9 shows data taken at 77 K and 13.73 GHz for Au/STO/LAO CMPS with STO films 300 nm and 1.0 μm thick, respectively. Note that for $|V_{dc}| \leq 260$ V, $\Delta\phi$ increases monotonically without any reversal. Also for the 1.0 μm film structure, $\Delta\phi$ is nearly three times larger than that measured for the structure with the 300 nm thick STO film. Thus, for the temperature, frequency, and bias stated above, a 360° CMPS with a 1.0 μm thick STO film could be nominally 4.0 mm long, and with a 300 nm thick STO the same CMPS would be nominally 12 mm long. These estimates assume that the passband would be maintained over the operating range. The experimental results obtained here are within less than a factor of two of the values for $\Delta\phi$ expected from theoretical predictions (see Table II).

TABLE II Theoretical insertion phase for coupled microstripline. (w = 76.2 μm, s = 12.7 μm) [Frequency = 13.0 GHz, L = 660 μm]

ε_{STO}	$\Delta\phi(t_{STO} = 0.3\ \mu m)$ deg.	$\Delta\phi(t_{STO} = 1.0\ \mu m)$ deg.
200	---	---
300	0.6	1.3
2000	6.7	17.4
3500	10.5	22.3
5000	13.7	28.7

Table III compare our results with those of others. Figure 9 also shows that, once again, replacing the Au film by the YBCO film resulted in larger $\Delta\phi$ values; this is presumably because of modified current distribution although more detailed analysis is required to fully account for this empirical behavior. As an additional advantage, tanδ does not seems to be a significant hindrance for the implementation of these phase shifters at K-band frequencies. Modeling of these structures by allowing tanδ of the substrate (i.e., STO and LAO as a whole) to be as high a 0.1, resulted in an insertion loss of less than 5 dB at 20 GHz and 77 K. For 700 nm thick BSTO (Ba:Sr; 0.4:0.6) thin films, the 25Ω Au/BSTO/LAO CMPS showed $\Delta\phi \sim 8° - 10°$ at 296 and 200 K, respectively, for $|V_{dc}|$ up to 160 V. The marginal performance suggests that further optimization of this material is required.

We have also investigated the performance of contiguous and interdigital ring resonators fabricated using Au/STO/LAO and YBCO/STO/LAO, respectively (figure 10). These resonators are intended for use in tunable discriminator-locked oscillators which could enhance the performance of LO for satellite communication systems, particularly by reducing the phase noise and consequently bit error rate (BER) degradation.[11,12] Figure 11 shows the magnitude of the transmission (S_{21}) and reflection (S_{11}) scattering parameters for Au/LAO and Au/STO/LAO ring resonators designed for operation at 20 GHz and with dimensions as given in figure 10. Observe that, as expected, there is slight shift in frequency (~2%) and a small increase (decrease) in insertion (return) loss due to the slight impedance change and loss tangent introduced by the STO layer. Figure 12 shows S_{21} versus temperature

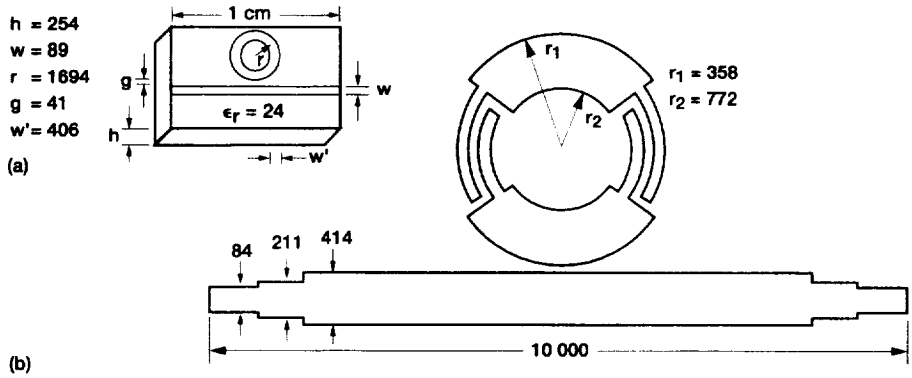

FIGURE 10 Au(1.5 μm thick)/STO (300 nm thick)/LAO (254 μm thick), 20 GHz ring resonators, (a) 25 Ohm ring, 50 Ohm transmission line, (b) 25 Ohm ring with interdigital gaps and input/output 50 to 25 Ohms transformer. All dimensions are in microns.

TABLE III Ferroelectric based phase shifters.

Material	Structure	T (K)	F (GHz)	Phase shift		Insertion loss (dB)	Return loss (dB)	E (10^4 V/cm)	Voltage (V)	Reference
				(Deg.)	(Deg/mm)					
BSTO (0.45:0.55), ceramic, 508 μm thick	Metal/Duroid ε_r = 2.2) & metal/ferroelectric (rod type) microstrip phase shifter, L = 6.550 mm	298	4.0	35	5.3	2.5 over a 20% band width	15	1.2	610	Babbitt, et al., Mic. Jour. 53, 1992
BSTO (0.6:0.4), 1.0 μm thick film on sapphire	CPW, with 0.5 μm metallization	298	35	47		10	--	--	20	L.C. Sengupta et al., Army Science Conf. 1996
STO, 2 μm thick film, PLD	CPW (YBCO (0.4 μm)/ STO/LAO (500 μm), L = 6.0 mm	77	2	15	2.5	-----	--	1.0	40	Findikoglu, et al., Micro. Opt. Tech. Lett., 9, 1995
STP, 1.0 μm thick film, PLD	YBCO Meander line CPW L = 25 cm; area: 1×1 cm (YBCO)	76	1	~100	0.44	<3 dB		0.25	5	Findikoglu, et al., ACS 1996
		76	2	~200	0.88	<3 dB		0.25	5	
		76	3	~300	13.3	<3 dB		0.25	5	
		76	1	~200	0.88	<3 dB		0.50	10	Findikoglu, et al., ACS 1996
		76	2	~400	1.78	<3 dB		0.50	10	Findikoglu, et al., ACS 1996
		76	3	~600	2.67	<3 dB		0.50	10	Findikoglu, et al., ACS 1996
BSTO (5% Ba), 960 nm thick film, PLD	CPW YBCO (300 nm)/ BSTO/LAO L = 4 mm	50	20	~40	10	~2.5	--	1.4	35	Gevorgian, et al., ACS 96
STO, 300 nm thick film, PLD	Interdigital Coupled lines AU (1.5 μm)/STO/LAO (254 μm), L = 0.66 mm	77	19.4	13	19.7			2.5	32	Miranda, et al., (This Conference)
STO, 300 nm thick film, PLD	Interdigial Coupled lines YBCO (35 μm)/STO/ LAO (254 μm), L = 0.66 mm	77	18.305	34	51.5	<2.2		2.5	32	Miranda, et al. (This Conference)

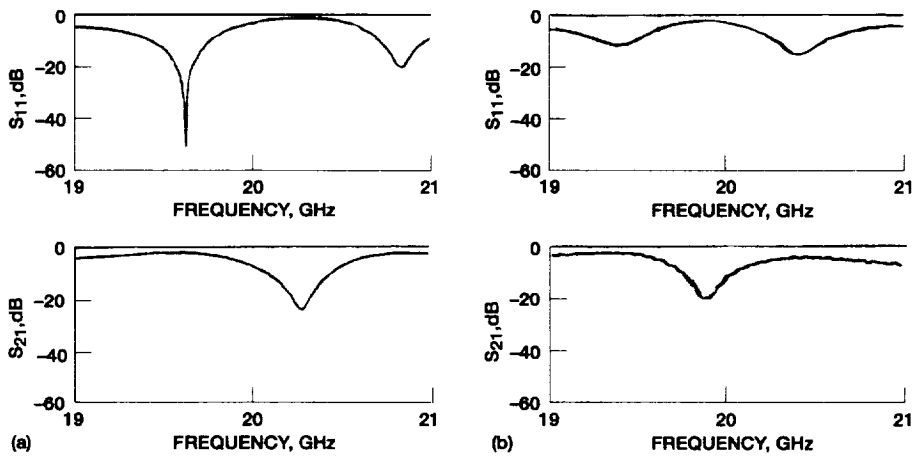

FIGURE 11 Transmission (S_{21}) and reflection (S_{11}) scattering parameters for (a) Au(1.5 μm)/ LAO (254 μm) and (b) Au(1.5 μm)/STO(300 nm)/LAO(254 μm) 25 Ohm ring resonators at room temperature. The power level was 10 dBm. ΔF = 2%, F = resonant frequency.

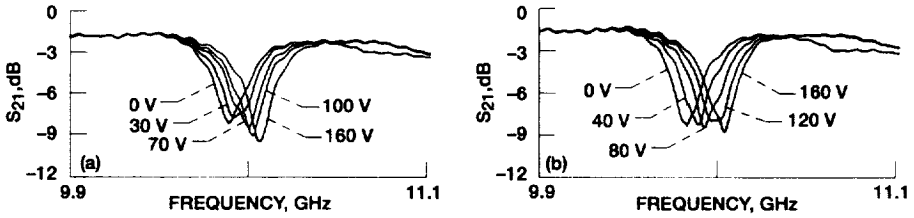

FIGURE 12 YBCO (350 nm)/STO (300 nm)/LAO (254 μm) 25 Ω, 2 λ ring resonators; (a) 77 K, (b) 50 K.

for a YBCO/STO(300 nm)/LAO 25 Ω, 2λ, interdigital ring resonator at 10 GHz. At 77 K, the resonant frequency of the resonator shifted by 110 MHz with a 160 V dc bias; at 50 K, the frequency shift was ~160 MHz. This resonator exhibited loaded and unloaded Q's of 54 and 110, respectively, at no bias, and of 55 and 160 at 160 V, as calculated using the method of Khanna and Garault.[13]

CONCLUSIONS

We have reported on the characterization of (metal, HTS)/STO/YBCO and (metal)/BSTO/LAO thin film multilayer structures in terms of the dielectric properties of the ferroelectric layer at frequencies up to 20 GHz. We have observed that the largest tuning of the Au/STO/YBCO parallel plate capacitors corresponds to single-phased, epitaxial

300-500 nm thick STO films deposited at 800 °C. Although the STO films in parallel plate configuration can be tuned with low dc bias (0-5 V), their performance is limited by the high effective tanδ. Higher dc voltages (tens of volts) are required to tune the interdigital structures, but their higher degree of tunability and lower tanδ make them attractive for microwave applications. We have developed proof-of-concept coupled microstrip lines phase shifters at 20 GHz, with low insertion loss and promising insertion phase shift per unit length. Implementation of these phase shifters with YBCO microstriplines resulted in greater phase shift per unit length than their metallic counterparts, presumably because of modified current distribution. These phase shifters are competitive with solid state-switched phase shifters in terms of performance and size, and promise simplicity of fabrication and cost advantage. For 2λ YBCO/STO ring resonators, unloaded Q's improved with bias and showed values of 110 and 160 at zero and 160 V, respectively. For this resonator a tuning rate of ~0.7 MHz/Volt was achieved at 77 K and 10 GHz. This type of ring resonator can be incorporated as a tunable element in a discriminator-locked oscillator. Optimization of this configuration and ring resonator configurations is currently underway.

Acknowledgments

One of the authors (F.W.V.K) gratefully acknowledges the support of the National Research Council.

References

[1.] V.K. Varadan, D.K. Ghodgaonkar, V.V. Varadan, J.K. Kelly, and P. Glikerdas, *Microwave Journal*, **35**, 116 (1992).

[2.] R.W. Babbit, T.E. Koscica, and W.C. Drach, *Microwave Journal*, **35**, 63 (1992).

[3.] D. Galt, J.C. Price, J.A. Beall, and R.H. Ono, *Appl. Phys. Lett.*, **63**, 3079 (1993).

[4.] G. Gilder, *Forbes ASAP*, Oct. 10 (1994).

[5.] F.A. Miranda, C.H. Mueller, C.D. Cubbage, K.B. Bhasin, R.K. Singh, and S. D. Harkness, *IEEE Trans. Appl. Supercond.*, **5**, 3191 (1995).

[6.] F.A. Miranda, C.H. Mueller, G.A. Koepf and R.M. Yandrofski, *Supercond. Sci. Technol.*, **8** , 755 (1995).

[7.] F.A. Miranda, C.H. Mueller, R.E. Treece, T.V. Rivkin, J.B. Thompson, H.R. Moutinho, M. Galberth, and C.T. Rogers, *Integrated Ferroelectrics*, **14**, 173 (1997).
[8.] C.H. Mueller, R.E. Treece, T.V. Rivkin, F.A. Miranda, H. R. Moutinho, A. Swartzlander-Franz, M. Dalberth, and C.T. Rogers, to be published in *IEEE Trans. Appl. Supercond.* (spring 1997).
[9.] S.K. Koul and B. Bhat, *IEEE MTT-S Digest*, 489 (1981).
[10.] R. Crampagne, M. Ahmadpanah, and J-L. Guiraud, *IEEE Trans. Microwave Theory Tech.*, **26**, 82 (1978).
[11.] Cheah, J.Y.C., *RF Design*, **11**, 99 (1991).
[12.] Howald, R.L., *Microwaves & RF*, **12**, 97 (1993).
[13.] A. Khanna and Y. Garault, *IEEE Trans. Microwave Theory Tech.*, **31**, 261 (1983).

REPORT DOCUMENTATION PAGE

Form Approved
OMB No. 0704-0188

1. AGENCY USE ONLY (*Leave blank*)	2. REPORT DATE	3. REPORT TYPE AND DATES COVERED
	May 1997	Technical Memorandum

4. TITLE AND SUBTITLE

Thin Film Multilayer Conductor/Ferroelectric Tunable Microwave Components for Communication Applications

5. FUNDING NUMBERS

WU-632-50-5D

6. AUTHOR(S)

Félix A. Miranda, Robert R. Romanofsky, Frederick W. Van Keuls, Carl H. Mueller, Randolph E. Treece, and Tania V. Rivkin

7. PERFORMING ORGANIZATION NAME(S) AND ADDRESS(ES)

National Aeronautics and Space Administration
Lewis Research Center
Cleveland, Ohio 44135-3191

8. PERFORMING ORGANIZATION REPORT NUMBER

E-10695-1

9. SPONSORING/MONITORING AGENCY NAME(S) AND ADDRESS(ES)

National Aeronautics and Space Administration
Washington, DC 20546-0001

10. SPONSORING/MONITORING AGENCY REPORT NUMBER

NASA TM-107456

11. SUPPLEMENTARY NOTES

Prepared for the 9th International Symposium on Integrated Ferroelectrics sponsored by the University of Colorado, Santa Fe, New Mexico, March 2–5, 1997. Félix A. Miranda, Robert R. Romanofsky, and Frederick W. Van Keuls, NASA Lewis Research Center; Carl H. Mueller, Randolph E. Treece and Tania V. Rivkin, SCT, Golden, Colorado 80401. Responsible person, Félix A. Miranda, organization code 5620, (216) 433–6589.

12a. DISTRIBUTION/AVAILABILITY STATEMENT

Unclassified - Unlimited
Subject Category 76

This publication is available from the NASA Center for AeroSpace Information, (301) 621-0390

12b. DISTRIBUTION CODE

13. ABSTRACT (***Maximum 200 words***)

High Temperature Superconductor/Ferroelectric (HTS/FE) thin film multilayered structures deposited onto dielectric substrates are currently being investigated for use in low loss, tunable microwave components for satellite and ground based communications. The main goal for this technology is to achieve maximum tunability while keeping the microwave losses as low as possible, so as to avoid performance degradation when replacing conventional technology (e.g., filters and oscillators) with HTS/FE components.Therefore, for HTS/FE components to be successfully integrated into current working systems, full optimization of the material and electrical properties of the ferroelectric films, without degrading those of the HTS film, is required. Hence, aspects such as the appropriate type of ferroelectric and optimization of the deposition conditions (e.g., deposition temperature) should be carefully considered. The tunability range as well as the microwave losses of the desired varactor (i.e., tunable component) are also dependent on the geometry chosen (e.g., parallel plate capacitor, interdigital capacitor, coplanar waveguide, etc.). In addition, the performance of the circuit is dependent on the location of the varactor in the circuit and the biasing circuitry. In this paper, we will present our results on the study of the $SrTiO_3/YBa_2Cu_3O_{7-\delta}/LaAlO_3$ (STO/YBCO/LAO) and the $Ba_xSr_{1-x}TiO_3/YBa_2Cu_3O_{7-\delta}/LaAlO_3$(BSTO/YBCO/LAO) HTS/FE multilayered structures. We have observed that the amount of variation of the dielectric constant upon the application of a dc electric field is closely related to the microstructure of the film. The largest tuning of the STO/YBCO/LAO structure corresponded to single-phased, epitaxial STO films deposited at 800° C and with a thickness of 500 nm. Higher temperatures resulted in interfacial degradation and poor film quality, while lower deposition temperatures resulted in films with lower dielectric constants, lower tunabilities, and higher losses. For STO/LAO multilayer structures having STO film of similar quality we have observed that interdigital capacitor configurations allow for higher tunabilities and lower losses than parallel plate configurations, but required higher dc voltage. Results on the use of these geometries in working microwave components such as filters and stabilizing resonators for local oscillators (LO) will be discussed.

14. SUBJECT TERMS	15. NUMBER OF PAGES
Ferroelectric films; HTS thin films; Dielectric constant; Loss tangent; K-factor; Phase shifters; Local oscillator	18
	16. PRICE CODE: A03

17. SECURITY CLASSIFICATION OF REPORT	18. SECURITY CLASSIFICATION OF THIS PAGE	19. SECURITY CLASSIFICATION OF ABSTRACT	20. LIMITATION OF ABSTRACT
Unclassified	Unclassified	Unclassified	